Fractions and fakeons in quantum field theory

Damiano Anselmi*

Dipartimento di Fisica "Enrico Fermi", Università di Pisa, Largo B. Pontecorvo 3, 56127 Pisa, Italy and INFN, Sezione di Pisa, Largo B. Pontecorvo 3, 56127 Pisa, Italy

(Received 14 June 2026; accepted 3 August 2026; published 9 September 2026)

We investigate formulations of quantum field theories whose kinetic terms involve fractional or continuous powers of the d'Alembert operator. The primary requirements are perturbative unitarity and a well-defined classical limit with a finite number of initial conditions. A direct approach consists of continuing the correlation functions from Euclidean space to Minkowski spacetime using the fakeon prescription for the fractional part of the power. Alternative formulations arise through decomposition, in which the fractional part is represented as a continuum of ordinary fakeons. These options are infinite in number and yield inequivalent Minkowskian theories with the same Euclidean counterpart. We demonstrate these features at tree level and for bubble diagrams. We also point out potential pitfalls in the calculations. Finally, we show how to treat continuous powers of covariant d'Alembertians in fractional gauge and gravity theories. The Ward and Cutkosky identities hold in all formulations.

DOI: 10.1103/75jy-gbbl

I. INTRODUCTION

Quantum field theory (QFT) remains by far the most successful framework for the description of high-energy phenomena. It forms the basis of the Standard Model of particle physics and has achieved an extraordinary level of agreement with experiments. While a variety of alternative approaches to fundamental interactions have been proposed in the past decades, none have yet matched the empirical success and internal consistency of QFT.

Despite its accomplishments, extending QFT beyond its standard domain or modifying its fundamental structures raises subtle conceptual and technical challenges. In this context, theories characterized by nonlocal or generalized kinetic operators have attracted considerable attention, starting with the pioneering works of Pais and Uhlenbeck [1] and Efimov [2]. Various developments have surfaced since then. Among these, we highlight the intriguing strategy pursued by Krasnikov, Kuz'min, Tomboulis, Modesto, and others over the years [3–8], which amounts to removing the ghost degrees of freedom of higher-derivative theories by inserting appropriate form factors. In this way, perturbative unitarity is achieved [9,10] and renormalizability is preserved [7,8]. Related investigations worth mentioning are those of [11].

Nevertheless, not everybody is comfortable with abandoning locality altogether. A different strategy was outlined by Lee and Wick at the end of the sixties [12], where the "abnormal particles" decay quickly enough to remain unobservable in most applications. Variants of this idea have been proposed in the past decade, involving propagators with complex poles [13], analogies with quantum chromodynamics [14], antilinear symmetries [15], and unstable ghosts [16].

A sort of intermediate option between locality and nonlocality is represented by purely virtual particles, or "fakeons", which are "particles" that are always off the mass shell [17]. One starts from a "parent" local theory and generates the "descendant" nonlocal fakeon theory by turning would-be ghosts or even nonproblematic particles into fake particles through certain diagrammatic operations and a projection on the asymptotic states [17–21]. This procedure yields a nonlocal quantum field theory of a special type, which can be renormalizable and unitary at the same time.

Fakeons leave observable imprints of various types. In quantum gravity, they lead to testable predictions about primordial cosmology by affecting the spectra of scalar and tensor fluctuations [22]. From the phenomenological point of view, they differ from resonances by exhibiting a pair of bumps rather than a peak [23]. Moreover, they trigger a violation of microcausality [24] through the breaking of time ordering at energies larger than the fakeon mass [21].

A further arena to explore departures from locality while preserving key structural properties of QFT is fractional quantum field theory [25–28], which involves rational or real powers of the d'Alembert operator. The main challenge

*Contact author: damiano.anselmi@unipi.it

Published by the American Physical Society under the terms of the Creative Commons Attribution 4.0 International license. Further distribution of this work must maintain attribution to the author(s) and the published article's title, journal citation, and DOI. Funded by SCOAP³.

posed by these models is to have unitarity and a consistent classical limit at the same time.

Calcagni and Rachwał were the first to use fakeons as tools to address the unitarity issue [26], through spectral representations of complex powers of the d'Alembert operator [27]. In Ref. [28], models of fractional quantum gravity were studied.

We also recall that models with continuum powers of kinetic operators, defined by means of the usual Feynman prescription, have been considered by Krasnikov [29] as particular cases of the notion of unparticle, introduced by Georgi in Ref. [30]. In those models, the issue of unitarity is addressed from the point of view of conformal field theory.

Here, we elaborate on fractional QFT in a general field theoretical spirit. We prove that fakeons can be employed in infinitely many inequivalent ways, starting from a "direct" formulation, which does not necessitate the use of spectral representations. Each option yields a different Minkowskian theory with the same Euclidean counterpart.

In the direct approach, the Minkowskian correlation functions are obtained by applying the fakeon prescription (via the so-called "average continuation" [17–19]) directly to the Euclidean ones.

The other formulations consist of converting the fractional powers of derivative operators into one-parameter families of ordinary fakeons through spectral decompositions. We analyze options not considered in the literature so far. A particular choice returns the results of the direct approach.

Depending on the decomposition itself, one obtains an infinite class of inequivalent models. We illustrate this explicitly at tree level and in loop diagrams, pointing out nontrivial aspects of the calculations, which may lead to erroneous results if fakeons are not dealt with by the book.

Fakeons ensure perturbative unitarity, which is expressed diagrammatically by the Cutkosky-Veltman identities [31]. Another requirement is that the theory admit a proper classical limit. This is not guaranteed, in general, since fractional powers of the d'Alembert operator may lead to nonreal or non-Hermitian kinetic terms. All formulations studied here admit a meaningful classical limit and propagate only the expected physical degrees of freedom. In particular, the nonlocal field equations are not burdened with the need to specify infinitely many initial conditions.

Finally, we show how to treat fractional or continuous powers of covariant d'Alembertians, in kinetic terms and vertices, to prove that the models can be consistently coupled to gauge fields and gravity. The Ward identities are satisfied in all formulations.

The paper is organized as follows. In Sec. II, we outline various options on the table to formulate fractional models, and show their inequivalence at tree level. In Sec. III, we calculate the bubble diagram in the simplest models and show that different formulations yield different results. In Sec. IV, more general fractional models are treated. Fractional powers of covariant d'Alembertians are handled in Sec. V. In Sec. VI, we prove that the set of degrees of freedom is the expected one. In Appendix A, we list simple properties of noninteger powers of a complex variable, while in Appendix B, we study the analytic continuation of the bubble diagram in the decomposition approach.

Square roots, logarithms, and noninteger powers are all taken on the principal branch. When a regularization technique is needed, we use the dimensional one [32], which aligns well with continuous powers of kinetic operators. Seen as complex parameters, they are at the core of the so-called analytic regularization [33], of which the dimensional one is the manifestly gauge-invariant upgrade.

II. MODELS WITH A FRACTIONAL D'ALEMBERTIAN

In this section we consider the simplest fractional models, based on the kinetic operator $\Box^\gamma$, comparing various options for their formulations. We introduce the direct approach, which has not appeared in the literature so far, and point out that it is not universally applicable. When it applies, we show how to retrieve equivalent results within the decomposition approach. Finally, we compare several QFT aspects of different decomposition formulations.

Let us start from the classical Lagrangians

$$\mathcal{L}_1 = -\frac{1}{2}\phi\Box^\gamma\phi - \frac{\lambda}{3!}\phi^3, \qquad \mathcal{L}_2 = -\frac{1}{2}\phi(\Box^2)^{\gamma/2}\phi - \frac{\lambda}{3!}\phi^3, \tag{2.1}$$

and assume $\gamma < 2$ to avoid infrared problems of the type $\sim \int \mathrm{d}^D p/(p^2)^\gamma$ in loop integrals around $d = 4$. We also assume $\gamma > 0$ to have propagators that tend to zero in the ultraviolet limit.

The theories (2.1) coincide in Euclidean space, since $\Box^\gamma = (-p_{\mathrm{M}}^2)^\gamma = (p_{\mathrm{E}}^2)^\gamma = [(p_{\mathrm{E}}^2)^2]^{\gamma/2} = [(-p_{\mathrm{M}}^2)^2]^{\gamma/2} = (\Box^2)^{\gamma/2}$ (where p_{M} and p_{E} are the Minkowski and Euclidean momenta, respectively), but differ in Minkowski spacetime. A shortcoming of the first Lagrangian is that it is not real for noninteger γ, at least if we interpret $\Box^\gamma$ as it stands. The classical equations of motion are

$$\Box^\gamma\phi + \frac{\lambda}{2}\phi^2 = 0, \tag{2.2}$$

and the propagator $-i/z^\gamma$, with $z = -p^2$, involves a fractional power that must be defined for $z < 0$. If we choose the branch cut on the negative real axis, the field equations are ill defined. If we choose it somewhere else, they are not real. The good news is that the fakeon approach is directly applicable to the Lagrangian $\mathcal{L}_1$ (see below).

The second theory leads to real classical equations of motion,

$$(\Box^2)^{\gamma/2}\phi + \frac{\lambda}{2}\phi^2 = 0. \tag{2.3}$$

Here we face a different type of problem. The complexification of the propagator, $-i/(z^2)^{\gamma/2}$, consists of two analytic functions with a cut along the imaginary axis; see Appendix A for details. This means that we cannot apply the fakeon approach as is, because it is based on the average continuation of *one* analytic function. Although generalizations might exist, we do not pursue them here.

The inherent differences between the two models suggest that they may lead to inequivalent theories in Minkowski spacetime, as we are going to show.

A. Direct fakeon approach

The direct fakeon approach is based on the "average continuation" [17–19] of the Euclidean amplitudes to Minkowski spacetime, which amounts to averaging the analytic continuations around the branch cuts involving fakeons. In the models we are considering, which do not propagate degrees of freedom, all the branch cuts are encompassed by the fakeon prescription.

This method is applicable to $\mathcal{L}_1$, but not to $\mathcal{L}_2$, because the propagator $-i/(z^2)^{\gamma/2}$ breaks the complex plane into two disjoint regions.

When we apply the average continuation to the $\mathcal{L}_1$ propagator, encoded into the function $f(z) = -i/z^\gamma$, the classical limit of $\mathcal{L}_1$ becomes acceptable. At first sight, it may seem unusual to advocate the average continuation already at tree level, but that is what one also does in local, nonfractional theories [17–19]. There, the operation is so simple that it basically goes unnoticed: acting on simple poles instead of cuts, it returns the Cauchy principal value $\mathcal{P}$, which defines the propagator "on the pole". For example, the average continuation of $1/p^2$ is $(1/2)[1/(p^2+i\epsilon) + 1/(p^2-i\epsilon)] = \mathcal{P}(1/p^2)$.

Writing $z = e^{i\theta}$ and noting that on the negative real axis

$$\frac{1}{2}\lim_{\theta\to\pi} e^{-i\gamma\theta} + \frac{1}{2}\lim_{\theta\to-\pi} e^{-i\gamma\theta} = \cos(\pi\gamma),$$

the $\mathcal{L}_1$ average-continued propagator in momentum space is

$$\begin{aligned} G_1(p^2) &= -\frac{i\theta(-p^2)}{(-p^2)^\gamma} - \cos(\pi\gamma)\frac{i\theta(p^2)}{(p^2)^\gamma} \\ &= -i\mathrm{Re}\left[\frac{1}{(-p^2-i\epsilon)^\gamma}\right]. \end{aligned} \tag{2.4}$$

For reference, the fakeon Green function in coordinate space, equal to the Fourier transform of $G_1(p^2)$, reads

$$\begin{aligned} \tilde{G}_1(x^2) &= \int \frac{d^D p}{(2\pi)^D} G_1(p^2) e^{-ip\cdot x} \\ &= -\frac{i\Gamma(\frac{D}{2}-\gamma)}{2^{2\gamma}\pi^{D/2}\Gamma(\gamma)}\mathrm{Re}\left[\frac{i}{(-x^2+i\epsilon)^{D/2-\gamma}}\right]. \end{aligned}$$

This result can be easily checked in the limit $\gamma \to 1$.

The effective action

$$\begin{aligned} \Gamma_1 = &-\frac{1}{2}\phi[\theta(\Box)\Box^\gamma + \sec(\pi\gamma)\theta(-\Box)(-\Box)^\gamma]\phi \\ &-\frac{\lambda}{3!}\phi^3 + \text{radiative corrections} \end{aligned} \tag{2.5}$$

makes sense for $\gamma \neq 1/2,\ 3/2$. For γ semi-integer Γ_1 is singular, so it is convenient to use the generating functional W_1 of connected Green functions, which is well defined.

At the level of radiative corrections, we proceed similarly by average-continuing the Euclidean diagrams and the correlation functions to Minkowski spacetime. At the practical level, it is convenient to use the dimensional regularization [32], where $D = d - \varepsilon$ denotes the complex spacetime dimension and d is the physical one. It is also convenient to treat γ as a complex parameter, in the spirit of the analytic regularization [33]. In this way, most loop integrals become ultraviolet convergent.

Consider, for example, the bubble diagram. In $d = 4$ dimensions, the associated integral is ultraviolet convergent for $1 < \gamma < 2$, and can be extended analytically to $0 < \gamma < 1$. We can assume $\gamma \neq 1$ and reach the case $\gamma \to 1$ as a limit. At the same time, if we keep the continued spacetime dimension D generic, the integral is ultraviolet convergent for $\gamma > D/4$.

The Euclidean result

$$B_{1\mathrm{E}}(p_\mathrm{E}^2) = c(p_\mathrm{E}^2)^{D/2-2\gamma}, \quad c = \frac{\lambda^2\Gamma(2\gamma-\frac{D}{2})\Gamma^2(\frac{D}{2}-\gamma)}{2(4\pi)^{D/2}\Gamma^2(\gamma)\Gamma(D-2\gamma)}, \tag{2.6}$$

leads to the Minkowskian outcome[1]

$$\begin{aligned} B_{1\,\mathrm{M}}(p^2) &= \frac{i}{2}[B_{1\mathrm{E}}(-p^2-i\epsilon) + B_{1\mathrm{E}}(-p^2+i\epsilon)] \\ &= ic\left[\theta(-p^2)(-p^2)^{D/2-2\gamma} + \cos\left(\frac{D\pi}{2} - 2\pi\gamma\right)\right. \\ &\quad \left.\times\,\theta(p^2)(p^2)^{D/2-2\gamma}\right]. \end{aligned} \tag{2.7}$$

The resummed (dressed) propagator reads

[1]We recall that a factor i must be included when the 1PI correlation functions are switched from the Euclidean framework to the Minkowski one in momentum space. The analytic continuation is $B_\mathrm{M}^{\mathrm{an}}(p^2) = iB_\mathrm{E}(-p^2-i\epsilon)$. The average continuation gives (2.7).

$$G_1^{\rm d}(p^2) = -\frac{i\theta(-p^2)}{(-p^2)^\gamma - c(-p^2)^{D/2-2\gamma}} - \frac{i\theta(p^2)\cos(\pi\gamma)}{(p^2)^\gamma - c\cos(\pi\gamma)\cos(\frac{D\pi}{2}-2\pi\gamma)(p^2)^{D/2-2\gamma}}.$$

We see that, consistent with unitarity in the fakeon approach, the result is purely imaginary. No physical degrees of freedom are on the external legs (by projection) and none is turned on by the radiative corrections (by the fakeon diagrammatics).

In the case of $\mathcal{L}_2$, we must search for a different formulation.

B. Decomposition approach

The decomposition approach consists of expressing the fractional propagator as a superposition of local propagators with complex poles, and treating those as fakeons inside diagrams. It can be applied to both theories (2.1). In the case of $\mathcal{L}_1$, it leads to the same results as the direct fakeon approach.

For $0 < \gamma < 1$, we can express the Euclidean $\mathcal{L}_1$ propagator by means of the spectral decomposition [34]

$$G_{1\rm E}(p_{\rm E}^2) = \frac{1}{(p_{\rm E}^2)^\gamma} = \int_0^\infty {\rm d}s\,\frac{\rho_\gamma(s)}{p_{\rm E}^2+s}, \qquad \rho_\gamma(s) = \frac{\sin(\pi\gamma)}{\pi s^\gamma}. \tag{2.8}$$

This expression is divergent for $1 < \gamma < 2$, where we can use

$$G_1(p_{\rm E}^2) = \int_0^\infty {\rm d}s\rho_\gamma(s)\left(\frac{1}{p_{\rm E}^2+s} - \frac{1}{p_{\rm E}^2}\right) \tag{2.9}$$

instead.

The diagrams must be evaluated in the Euclidean framework, keeping the s-parameters fixed. Then, one performs the average continuation to Minkowski spacetime on the integrands of the s-integrals. Finally, one integrates over the s-parameters.

Alternatively, one can apply the fakeon diagrammatics of refs. [20,21] directly in Minkowski spacetime. This means:

(1) Calculate the usual Feynman diagrams with the $i\epsilon$ propagators, i.e.,

$$\int_0^\infty {\rm d}s\,\frac{i\rho_\gamma(s)}{p^2-s+i\epsilon}, \qquad \int_0^\infty {\rm d}s\rho_\gamma(s)\left(\frac{i}{p^2-s+i\epsilon} - \frac{i}{p^2+i\epsilon}\right), \tag{2.10}$$

for the cases $0 < \gamma < 1$ and $1 < \gamma < 2$, respectively, and combine them in a prescribed way (which can be found in [20,21]) with additional diagrams built with (2.10) and the "cut propagators"

$$\int_0^\infty {\rm d}s\rho_\gamma(s)(2\pi)\theta(\pm p^0)\delta(p^2-s), \qquad \int_0^\infty {\rm d}s\rho_\gamma(s)(2\pi)\theta(\pm p^0)[\delta(p^2-s)-\delta(p^2)]. \tag{2.11}$$

(2) Evaluate the diagrams at fixed parameters s, using the dimensional regularization and keeping the continued dimension D generic; this means that no renormalization and no expansion of D around the physical dimension d must be performed at this stage (see below for examples in calculations).
(3) Evaluate the integrals on the s-parameters.
(4) Expand D around the physical value d and, if needed, renormalize the divergent parts.

In particular, the free two-point functions (2.4) are

$$G_1(p^2) = \mathcal{P}\int_0^\infty {\rm d}s\rho_\gamma(s)\frac{i}{p^2-s}, \qquad G_1(p^2) = \mathcal{P}\int_0^\infty {\rm d}s\rho_\gamma(s)\left(\frac{i}{p^2-s} - \frac{i}{p^2}\right), \tag{2.12}$$

for $0 < \gamma < 1$ and $1 < \gamma < 2$, respectively.

Note that the sign of the spectral density is not relevant to the discussion of this paper, since fakeons can accommodate both signs.

It is important that the subtraction of counterterms (if needed) not be performed at fixed parameters s, since the s-integrals may generate additional divergences or cancel out the spurious ones. Yet, the finite parts of the diagrams may turn out to be correct nonetheless. In the next section, we illustrate these points explicitly in the bubble case.

A fact to keep in mind is that the fakeon diagrammatics does not amount to computing Feynman diagrams with an alternative propagator (which would be (2.8) or (2.9) in the decomposition approach, (2.4) in the direct approach). This option has been studied in the past [35] and leads to violations of unitarity. Details on the difference between the two approaches in ordinary, non-fractional models (which is already visible in the bubble diagram) can be found in Ref. [36].

For $\mathcal{L}_2$, we write

$$G_{2\rm E}(p^2) = \frac{1}{[(p_{\rm E}^2)^2]^{\gamma/2}} = \int_0^\infty {\rm d}s\,\frac{\rho_{\gamma/2}(s)}{(p_{\rm E}^2)^2+s}. \tag{2.13}$$

Note that $0 < \gamma/2 < 1$ implies that the integral is IR and UV convergent. The calculation of diagrams proceeds as described above.

In general, a fakeon decomposition, such as (2.8)–(2.9) and (2.13), and the average continuation are operations that may not commute. This is already evident at tree level, since $\mathcal{L}_1$ and $\mathcal{L}_2$ coincide in Euclidean space (the functions $-i/z^\gamma$ and $-i/(z^2)^{\gamma/2}$ being identical for ${\rm Re}[z] > 0$), but

lead to different propagators in Minkowski spacetime, i.e., (2.4) versus

$$G_2(p^2) = -\frac{i}{[(-p^2)^2]^{\gamma/2}}. \tag{2.14}$$

Thus, caution must be used before commuting the two operations at the level of diagrams. In the next section, we prove that $\mathcal{L}_1$ and $\mathcal{L}_2$ give different results for the bubble diagram.

1. Model 1 and Model 2 face to face

As said, the two models are identical in Euclidean space, yet different in Minkowski spacetime. This discrepancy arises from the *continuous* sector of the decomposition, which can be dealt with in an infinite number of ways. The outcome is an infinite family of inequivalent theories.

Let us summarize the situation so far, focusing on the case $0 < \gamma < 1$ for simplicity. In Euclidean space, we have

$$\frac{1}{(p_{\rm E}^2)^\gamma} = \int_0^\infty \mathrm{d}s \frac{\rho_\gamma(s)}{p_{\rm E}^2 + s}, \qquad \frac{1}{[(p_{\rm E}^2)^2]^{\gamma/2}} = \int_0^\infty \mathrm{d}s \frac{\rho_{\gamma/2}(s)}{(p_{\rm E}^2)^2 + s}. \tag{2.15}$$

The two expressions coincide for $z = p_{\rm E}^2 > 0$, but give different results when we turn to Minkowski spacetime (by performing the substitution $p_{\rm E}^2 \to -p^2 - i\epsilon$ plus the average continuation). If we choose the density $\rho_\gamma(s)$, we have a continuum of fakeons with square masses equal to s. If we choose the density $\rho_{\gamma/2}(s)$, we have a continuum of complex conjugate fakeon pairs with square masses equal to $\pm i\sqrt{s}$.

Now, consider the formula

$$\frac{1}{[(p_{\rm E}^2)^n]^{\gamma/n}} = \int_0^\infty \mathrm{d}s \frac{\rho_{\gamma/n}(s)}{(p_{\rm E}^2)^n + s}, \qquad n \in \mathbb{N}_+. \tag{2.16}$$

The lefthand sides of this equality are all equal to $(p_{\rm E}^2)^{-\gamma}$ in Euclidean space. Yet, different values of n lead to different Minkowskian theories.

For example, the Minkowski expressions

$$\int_0^\infty \mathrm{d}s \frac{\rho_{\gamma/n}(s)}{(-p^2 - i\epsilon)^n + s} = \frac{1}{[(-p^2 - i\epsilon)^{2k+1}]^{\gamma/(2k+1)}} \tag{2.17}$$

differ from one another for odd $n = 2k + 1$, $k \in \mathbb{N}$, to the extent that the average continuation

$$\left.\frac{1}{[(-p^2 - i\epsilon)^{2k+1}]^{\gamma/(2k+1)}}\right|_{\rm f} = \frac{\theta(-p^2)}{(-p^2)^\gamma} + \cos\left(\frac{\pi\gamma}{2k+1}\right)\frac{\theta(p^2)}{(p^2)^\gamma} \tag{2.18}$$

(where the subscript "f" means "fakeon") is k dependent.

Note that in the complex plane $p_{\rm E}^2 \to z = \rho e^{i\theta}$, the function on the lefthand side of (2.16) has cuts in the radii $\theta =$ odd multiple of π/n. This means that the plane is divided into disjoint regions for all $n > 1$, which makes the direct fakeon approach applicable only for $n = 1$.

For all even values of n, formulas (2.17) give the same result, which is (2.13) times i. Nevertheless, the calculations of the next section (where we show that the options (2.15) give different results for the bubble diagram) suggest that the radiative corrections are all different in those cases as well.

The conclusion is that different decompositions lead to different theories. Since infinitely many options are available, infinitely many inequivalent fractional theories correspond to the same Euclidean model.

C. Non-Hermitian formulation

The most natural option to make sense of kinetic terms involving fractional powers of the D'Alembertian operator is to decompose the propagator as a continuum of standard particles, rather than fakeons, treating the poles by means of the Feynman $i\epsilon$ prescription [26]. We have left this approach for last because it does not satisfy our requirements.

Specifically, the strategy amounts to using the Källén–Lehmann representation

$$G_3(p^2) = -\frac{i}{(-p^2 - i\epsilon)^\gamma} = i\int_0^\infty \mathrm{d}s \frac{\rho_\gamma(s)}{p^2 - s + i\epsilon}$$

(still at $0 < \gamma < 1$). The resulting theory is unitary, since the Cutkosky-Veltman equations are obeyed. However, the classical equations of motion

$$(\Box - i\epsilon)^\gamma \phi + \frac{\lambda}{2}\phi^2 = 0$$

are not real. Because of this, we do not pursue this formulation further in this paper.

III. DIAGRAMMATICS

In this section, we study the diagrammatics of fractional models and show that different formulations lead to different results for the same contribution to an amplitude.

As recalled, the fakeon diagrammatics involves a combination of Feynman diagrams and additional diagrams built with both Feynman and cut propagators. In the case of the bubble, the procedure amounts to applying a simple operation ("fakeon prescription") on the usual integral. Precisely, one starts from the Euclidean loop integral and "average-continues" it to Minkowski spacetime, i.e., averages the analytic continuations around the branch cut.

In the direct fakeon approach, one can apply the average continuation on the Euclidean result (2.6), which gives (2.7). In the decomposition approach, one has to apply it for fixed parameters s and integrate over them at the end. This is what we do explicitly in the next subsections.

A. Model 1

Let us take $0 < \gamma < 1$ for the moment. Using the left decomposition of (2.10), the bubble diagram gives the loop integral

$$\frac{\lambda^2}{2}\int_0^\infty \mathrm{d}s\rho_\gamma(s)\int_0^\infty \mathrm{d}\sigma\,\rho_\gamma(\sigma) \times \int \frac{\mathrm{d}^D k}{(2\pi)^D}\frac{1}{(k^2 - s + i\epsilon)((p+k)^2 - \sigma + i\epsilon)}. \quad (3.1)$$

The fakeon diagrammatics at fixed s and σ demands to average this expression with the one obtained by replacing $+i\epsilon$ with $-i\epsilon$. We discuss this later.

Using Feynman parameters, formula (3.1) gives

$$\frac{i\lambda^2}{2}\frac{\Gamma(2-\frac{D}{2})}{(4\pi)^{D/2}}\int_0^1 \mathrm{d}x\int_0^\infty \mathrm{d}s\rho_\gamma(s)\int_0^\infty \mathrm{d}\sigma\rho_\gamma(\sigma)(-p^2x(1-x) + sx + \sigma(1-x) - i\epsilon)^{D/2-2}. \quad (3.2)$$

The Schwinger representation

$$\frac{1}{A^\alpha} = \frac{1}{\Gamma(\alpha)}\int_0^\infty \mathrm{d}t\, t^{\alpha-1}\mathrm{e}^{-tA}, \qquad \mathrm{Re}[A] > 0, \qquad \mathrm{Re}[\alpha] > 0,$$

allows us to write it as

$$\frac{i\lambda^2(-i)^{D/2-2}}{2(4\pi)^{D/2}}\int_0^1 \mathrm{d}x\int_0^\infty \mathrm{d}t\, t^{1-\frac{D}{2}}\mathrm{e}^{-t\epsilon + ip^2tx(1-x)} \times \int_0^\infty \mathrm{d}s\,\rho_\gamma(s)\mathrm{e}^{-its x}\int_0^\infty \mathrm{d}\sigma\,\rho_\gamma(\sigma)\mathrm{e}^{-it\sigma(1-x)},$$

after which the s- and σ-integrals are straightforward. Using the identity

$$\int_0^\infty \mathrm{d}s\,\rho_\gamma(s)\mathrm{e}^{-its x} = \frac{(itx)^{\gamma-1}}{\Gamma(\gamma)}, \qquad 0 < \gamma < 1, \quad (3.3)$$

we obtain

$$\frac{i\lambda^2(-i)^{D/2}i^{2\gamma}}{2(4\pi)^{D/2}\Gamma^2(\gamma)}\int_0^1 \mathrm{d}x\, x^{\gamma-1}(1-x)^{\gamma-1} \times \int_0^\infty \mathrm{d}t\, t^{2\gamma-1-\frac{D}{2}}\mathrm{e}^{-t\epsilon + itp^2x(1-x)}.$$

At this point, the t-integral (defined by taking advantage of the dimensional regularization in D) yields

$$\frac{i\lambda^2}{2(4\pi)^{D/2}}\frac{\Gamma(2\gamma-\frac{D}{2})}{\Gamma^2(\gamma)}(-p^2 - i\epsilon)^{\frac{D}{2}-2\gamma}\int_0^1 \mathrm{d}x(x(1-x))^{\frac{D}{2}-\gamma-1},$$

having rescaled ϵ by $x(1-x)$. Finally, the x integral gives

$$\frac{i\lambda^2}{2(4\pi)^{D/2}}\frac{\Gamma(2\gamma-\frac{D}{2})\Gamma^2(\frac{D}{2}-\gamma)}{\Gamma^2(\gamma)\Gamma(D-2\gamma)}(-p^2 - i\epsilon)^{\frac{D}{2}-2\gamma}.$$

Once we sum the expression with $-p^2 - i\epsilon \to -p^2 + i\epsilon$ and divide by 2, we find agreement with (2.6).

For $1 < \gamma < 2$, we use the right decomposition of (2.10) and proceed in the same way. Instead of (3.3), we need the identity

$$\int_0^\infty \mathrm{d}s\,\rho_\gamma(s)(\mathrm{e}^{-its x} - 1) = \frac{(itx)^{\gamma-1}}{\Gamma(\gamma)}, \qquad 1 < \gamma < 2, \quad (3.4)$$

and the final result is the same.

The case $\gamma \to 1$ can be reached as a limit. There, we have to subtract the usual ultraviolet divergence in four dimensions.

Before proceeding, we highlight some potential pitfalls. In the decomposition approach, the bubble diagram of the fractional model is viewed as a continuum of ordinary bubble diagrams. However, the latter are divergent in $D = 4$ (check the last integral of (3.1)), while the former is convergent for every $\gamma \neq 1$. It is risky to expand $D = 4 - \varepsilon$ around its physical value $d = 4$ and throw away the divergent part in ε *before* integrating over s and σ. Those integrals may generate divergent parts that are out of control. Yet, if they are independent of the external momenta, as occurs in the case of the bubble diagram, the finite part turns out to be right.

Let us verify this explicitly. We expand the integrand of (3.2) for ε small, throw away the pole $1/\varepsilon$, and focus on the convergent part, as we would normally do. Then, we get

$$-\frac{i\lambda^2}{2(4\pi)^2}\int_0^1 \mathrm{d}x\int_0^\infty \mathrm{d}s\,\rho_\gamma(s)\int_0^\infty \mathrm{d}\sigma\,\rho_\gamma(\sigma) \times \ln(-p^2x(1-x) + sx + \sigma(1-x) - i\epsilon). \quad (3.5)$$

The s- and σ-integrations diverge, but their divergent parts are p-independent. We get rid of them by differentiating (3.5) with respect to p^2, using the procedure outlined above (Schwinger representation plus identities (3.3) and (3.4)), integrating back over p^2 and ignoring the p-independent additive constants. We obtain

$$\frac{i\lambda^2}{2(4\pi)^2}\frac{\Gamma^2(2-\gamma)\Gamma(2\gamma-2)}{\Gamma^2(\gamma)\Gamma(2\gamma)}(-p^2 - i\epsilon)^{2-2\gamma}, \quad (3.6)$$

which matches (2.6) for $D = 4$.

Since we know that there are no divergent parts for $\gamma \neq 1$, and the result must be proportional to $(-p^2 - i\epsilon)^{2-2\gamma}$ in $D = 4$ (on dimensional grounds), we conclude that (3.6) is complete: the additive constant we are missing is equal to zero.

What has happened? The corrections of higher orders in ε (originated by the expansion of D around $d=4$) have the form (3.5) with powers of ε in front and higher powers of the logarithm inside. All such integrals are convergent as soon as they are differentiated with respect to p^2. Hence, their contributions are killed by the limit $\varepsilon \to 0$.

Ultimately, the sector we are missing with this procedure is made of p-independent divergences, so the p-dependence of the finite part turns out to be correct. Moreover, the divergent parts must sum to zero, since the original integral was convergent.

Note that curious interplay between analytic [33] and dimensional [32] regularization techniques. The former views γ as a complex exponent. A loop integral is evaluated in an open set of the γ plane where it is convergent. Then the result is analytically continued to the physical value γ^* of γ. The divergent parts are negative powers of $\gamma-\gamma^*$.

In summary, the Lagrangian $\mathcal{L}_1$ admits two equivalent formulations, which also provide two options for the calculations: the direct fakeon approach and the decomposition approach. A drawback of the latter is that some caution must be used in order to properly deal with the (possibly spurious) divergent parts.

B. Model 2

In Model 2, we cannot apply the direct fakeon approach, so we rely on the decomposition strategy. The method of calculation described above extends straightforwardly, but calculations are more involved.

Let us highlight the main question we need to answer. In formulas (2.6) and (2.7), we had a single cut on the complex plane, so the average continuation was straightforward. Here instead, we have a single cut on the complex plane at fixed s and σ, but the integrals with respect to those variables can generate further cuts that divide the complex p^2 plane into disjoint regions. Hence, instead of (2.7), we expect a Minkowskian result of the form

$$B_{2\mathrm{M}}(p^2) = ic[\theta(-p^2)(-p^2)^{D/2-2\gamma} + g(\gamma)\theta(p^2)(p^2)^{D/2-2\gamma}], \tag{3.7}$$

where $g(\gamma)$ is a new function of γ. We may even have a different coefficient $g(\gamma)$ for every choice of n in (2.16). The results we derive below show precisely this. In particular, the case $n=2$ does not give the $n=1$ result (2.7), which is $g(\gamma)=\cos(\pi D/2-2\pi\gamma)$.

The $n=2$ Euclidean loop integral is

$$B_{2\mathrm{E}}(p_{\mathrm{E}}^2) = \frac{\lambda^2}{2}\int_0^\infty \mathrm{d}s\,\rho_{\gamma/2}(s)\int_0^\infty \mathrm{d}\sigma\,\rho_{\gamma/2}(\sigma)\int \frac{\mathrm{d}^D k_{\mathrm{E}}}{(2\pi)^D}\frac{1}{(k_{\mathrm{E}}^2)^2+s}\frac{1}{((p_{\mathrm{E}}+k_{\mathrm{E}})^2)^2+\sigma}. \tag{3.8}$$

Here, there are no ultraviolet divergences at fixed s and σ in $D<8$, so we can work directly in the physical dimension d.

Clearly, the Euclidean result is still (2.6). Hence, for $p^2<0$, the Minkowski one is

$$B_{2\mathrm{M}}(p^2) = iB_{2\mathrm{E}}(-p^2) = iB_{1\mathrm{E}}(-p^2) \qquad (p^2<0). \tag{3.9}$$

After replacing s and σ with s^2 and σ^2 in (3.8), respectively, we find

$$B_{2\mathrm{E}}(p_{\mathrm{E}}^2) = \frac{\lambda^2}{2(4\pi)^2}\int_0^\infty \mathrm{d}s\,\rho_{\gamma/2}(s^2)\int_0^\infty \mathrm{d}\sigma\,\rho_{\gamma/2}(\sigma^2)\int_0^1 \mathrm{d}x\,\ln\frac{(p_{\mathrm{E}}^2)^2x^2(1-x)^2+(xs+(1-x)\sigma)^2}{(p_{\mathrm{E}}^2)^2x^2(1-x)^2+(xs-(1-x)\sigma)^2} \tag{3.10}$$

in $d=4$ and

$$B_{2\mathrm{E}}(p_{\mathrm{E}}^2) = -\frac{\lambda^2}{8\pi}\int_0^\infty \mathrm{d}s\,\rho_{\gamma/2}(s^2)\int_0^\infty \mathrm{d}\sigma\,\rho_{\gamma/2}(\sigma^2)\int_0^1 \mathrm{d}x\left[\frac{1}{p_{\mathrm{E}}^2x(1-x)-ixs-i(1-x)\sigma} - \frac{1}{p_{\mathrm{E}}^2x(1-x)-ixs+i(1-x)\sigma}+\mathrm{c.c.}\right] \tag{3.11}$$

in $d=2$.

To simplify the calculation enough without missing the main point, we study the case $d=2$ for $1/2<\gamma<1$, where the integral of each contribution in the brackets of (3.11) is separately convergent. An analogous procedure can be applied to the case $d=4$ after differentiating (3.10) with respect to p_{E}^2. There, however, the integrals of the various contributions do not converge separately.

The next step is to make the average continuation of (3.11) at fixed s and σ. We give two procedures to achieve this goal: the first one, done below, amounts to studying the x-integral without calculating it. The second one, done in

Appendix B, amounts to continuing the result of the x-integral.

For s and σ generic, the expression

$$f(z,s,\sigma)=\int_0^1 \mathrm{d}x\left[\frac{1}{zx(1-x)-ixs+i(1-x)\sigma}+\frac{1}{zx(1-x)+ixs-i(1-x)\sigma}\right] \tag{3.12}$$

defines an analytic function of z in the half plane $\mathrm{Re}[z]>0$. Note that $f(z,s,\sigma)$ is real for real z, and symmetric with respect to the exchange $s\leftrightarrow\sigma$. Finally, it is odd in z:

$$f(-z,s,\sigma)=-f(z,s,\sigma). \tag{3.13}$$

We consider the contributions in the brackets separately. Each one is regular for $\mathrm{Re}[z]\neq 0$. Singularities may occur when z is purely imaginary.

It is convenient to divide the complex plane into the regions $\mathrm{Re}[z]>0$ and $\mathrm{Re}[z]<0$. Starting from the half plane $\mathrm{Re}[z]>0$ (which is the Euclidean region), our goal is to analytically continue $f(z,s,\sigma)$ to the half plane $\mathrm{Re}[z]<0$. For definiteness, we switch from $\mathrm{Re}[z]>0$ to $\mathrm{Re}[z]<0$ on the upper half plane.

The first denominator vanishes at the points

$$x_\pm=\frac{1}{2}-i\frac{s+\sigma}{2z}\pm\frac{i}{2z}\sqrt{(s+\sigma+iz)^2-4iz\sigma}.$$

When z crosses the positive imaginary axis, only x_+ crosses the integration domain $0\le x\le 1$, and it does so from below. This means that the analytic continuation of $f(z,s,\sigma)$ to $\mathrm{Re}[z]<0$ is $f(z,s,\sigma)$ plus the contribution of the residue at x_+.

Something similar happens with the second denominator. At the end, we have the analytic continuation

$$f^{\mathrm{an}}(z,s,\sigma)=\begin{cases} f(z,s,\sigma) & \text{for } \mathrm{Re}[z]>0 \text{ (Euclidean result)},\\ -f(-z,s,\sigma)+h(z,s,\sigma) & \text{for } \mathrm{Re}[z]<0,\end{cases} \tag{3.14}$$

where

$$h(z,s,\sigma)=\frac{2\pi}{\sqrt{(s+\sigma+iz)^2-4iz\sigma}}+\frac{2\pi}{\sqrt{(s+\sigma-iz)^2+4iz\sigma}}. \tag{3.15}$$

The imaginary axis can be reached from both directions.

To calculate (3.11), we also need to consider the integral

$$g(z,s,\sigma)=\int_0^1 \mathrm{d}x\left[\frac{1}{zx(1-x)-ixs-i(1-x)\sigma}+\frac{1}{zx(1-x)+ixs+i(1-x)\sigma}\right] \tag{3.16}$$

for generic s and σ. Again, $g(-z,s,\sigma)=-g(z,s,\sigma)$.

Studying the values of z for which the denominators vanish in the x-integration domain, it is easy to check that $g(z,s,\sigma)$ is an analytic function of z in a "safe" open strip containing the real axis, extending by an amount equal to $(\sqrt{s}+\sqrt{\sigma})^2$ above and below the real axis itself. Hence, the analytic continuation from the positive real axis to the negative one is straightforward. We have

$$g^{\mathrm{an}}(z,s,\sigma)=\begin{cases} g(z,s,\sigma) & \text{for } \mathrm{Re}[z]>0,\\ -g(-z,s,\sigma) & \text{for } \mathrm{Re}[z]>0.\end{cases} \tag{3.17}$$

Finally, the analytic continuation of (3.11) at fixed s and σ gives

$$B_{2\mathrm{E}}^{\mathrm{an}}(z)=-\frac{\lambda^2}{8\pi}\int_0^\infty \mathrm{d}s\,\rho_{\gamma/2}(s^2)\int_0^\infty \mathrm{d}\sigma\,\rho_{\gamma/2}(\sigma^2)[g^{\mathrm{an}}(z,s,\sigma)-f^{\mathrm{an}}(z,s,\sigma)]. \tag{3.18}$$

Note that, although the integrand is analytic by construction, the integral $B_{2\mathrm{E}}^{\mathrm{an}}(z)$ need not be an analytic function.

An unexpected property, which emerges from the calculation, is that the average continuation is automatically implemented by the integrals with respect to s and σ. In some sense, the decomposition approach knows about fakeons by default. Due to this, the Minkowski bubble diagram evaluates to

$$B_{2\mathrm{M}}(p^2)=iB_{2\mathrm{E}}^{\mathrm{an}}(-p^2)=\begin{cases} ic'(-p^2)[(-p^2)^2]^{-\gamma} & \text{for } p^2<0,\\ -B_{2\mathrm{M}}(-p^2)+\Delta B_{2\mathrm{M}}(p^2) & \text{for } p^2>0,\end{cases} \tag{3.19}$$

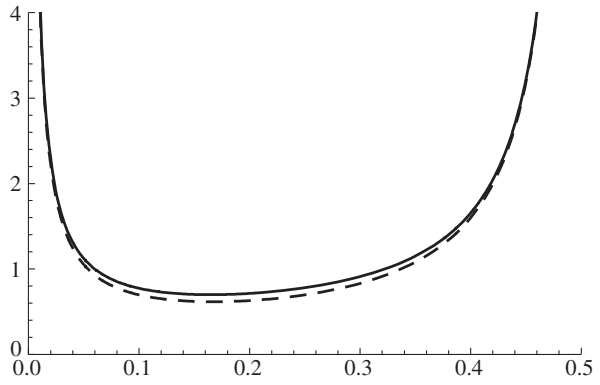


FIG. 1. Numerical comparison between $-2iB_{2M}(1)/\lambda^2$ (thick plot) and $-2iB'_{2M}(1)/\lambda^2$ (dashed plot) as functions of $\delta=\gamma-1/2$ for $0<\delta<1/2$.

where

$$c'=\frac{\lambda^2\Gamma(2\gamma-1)\Gamma^2(1-\gamma)}{2(4\pi)\Gamma^2(\gamma)\Gamma(2-2\gamma)},$$
$$\Delta B_{2M}(-z)=\frac{i\lambda^2}{8\pi}\int_0^\infty ds\,\rho_{\gamma/2}(s^2)\int_0^\infty d\sigma\,\rho_{\gamma/2}(\sigma^2)h(z,s,\sigma). \tag{3.20}$$

On dimensional grounds, we know that the final result has the form (3.7).

We do not have the explicit result for ΔB_{2M}, but for $p^2>0$ we can compare $B_{2M}(p^2)$ numerically to (2.7) and another simple option, which is

$$B'_{2M}(p^2)=ic'[\theta(-p^2)(-p^2)^{1-2\gamma}+\theta(p^2)(p^2)^{1-2\gamma}]$$
$$=ic'[(p^2)^2]^{1/2-\gamma}.$$

Figure 1 $-2iB_{2M}(p^2)/\lambda^2$ and $-2iB'_{2M}(p^2)/\lambda^2$ for $p^2=1$ as functions of $\delta=\gamma-1/2$. The result is that the coefficient $g(\gamma)$ of formula (3.7) is close to 1 for all values of γ in the range we are considering. However, it is not precisely 1. For example, we find $g(2/3)\simeq 1.45$, $g(3/4)\simeq 1.12$ and $g(5/6)\simeq 1.08$.

The difference with respect to (2.7) is more apparent, since $-\cos(2\pi\gamma)$ changes sign between $\gamma=1/2$ and $\gamma=1$.

Formulas (3.15), (3.19), and (3.20) show that ΔB_{2M} is purely imaginary, which is what we expect from the average continuation. Yet, we have derived it from $B^{an}_{2E}(z)$, formula (3.18), which comes from the analytic continuation of $B_{2E}(z)$ at fixed s and σ.

The fact, mentioned earlier, is that the analytic continuation of $B_{2E}(z)$ at fixed s and σ automatically turns into the average continuation after integrating over s and σ. Let us explain why.

By formula (3.15), the cuts of $h(z,s,\sigma)$ are located at $z=z_\pm$, where

$$z_\pm=i(s-\sigma)\pm\sqrt{u+4s\sigma},\qquad u\geqslant 0.$$

Only z_- is relevant for us, since the function $h(z,s,\sigma)$ contributes just for $\mathrm{Re}[z]<0$. This is a horizontal half line on the complex z plane, which crosses the real axis when $s-\sigma$ flips sign. It is evident that the s- and σ-integrations average the contributions where the squared momentum $p^2=-z\in\mathbb{R}$ is symmetrically placed above and below the z_- cut, which is what the average continuation prescribes. Hence, (3.19) is the final result.

Once again, we confirm that different decompositions lead to different fractional quantum field theories, although the Euclidean counterpart is the same.

Finally, combining (2.14) and (3.7), we find the dressed two-point function

$$G^d_2(p^2)=-\frac{i\theta(-p^2)}{(-p^2)^\gamma-c(-p^2)^{D/2-2\gamma}}$$
$$-\frac{i\theta(p^2)}{(p^2)^\gamma-cg(\gamma)(p^2)^{D/2-2\gamma}}.$$

1. Remark

We have found that the decomposition approach knows about fakeons by default, in the form of the average continuation. At the computational level, the reason is that the unusual, fractional propagator is replaced by a continuum of standard, local propagators, thereby providing regions where the cuts of the bubble diagram are placed both above and below the real axis, prior to integrating over s and σ. Hence, the integrations average the analytic continuations from above and below, as per the average continuation. Yet, it is remarkable that there is no need to enforce this as an external prescription.

This raises several questions which deserve further scrutiny. For example, it remains to be seen whether other diagrams exhibit the same property. Another interesting direction is to investigate to what extent it makes sense to view fakeons in local theories (where the prescription is a choice) as limits of the "natural fakeons" of fractional theories when the fractional power approaches an integer.

IV. EXTENDED MODELS WITH A FRACTIONAL D'ALEMBERTIAN

So far we have focused on simple models like (2.1), but it is clear that the direct fakeon approach and the decomposition approach are general. In this section, we illustrate extended models described by Lagrangians of the forms

$$\mathcal{L}_1=-\frac{1}{2}\phi\Box\left(1+\frac{\Box^\gamma}{M^{2\gamma}}\right)\phi+\mathcal{L}_{\rm int},$$
$$\mathcal{L}_2=-\frac{1}{2}\phi\Box\left(1+\left(\frac{\Box^2}{M^4}\right)^{\gamma/2}\right)\phi+\mathcal{L}_{\rm int},$$

where $\gamma>0$, and $\mathcal{L}_{\rm int}$ denotes generic self interactions.

A. Model 1

As before, the classical $\mathcal{L}_1$ field equations

$$\Box\left(1+\frac{\Box^\gamma}{M^{2\gamma}}\right)\phi = I_{\rm int}, \tag{4.1}$$

where $I_{\rm int}$ denotes interactions, are not acceptable, since they are ill defined or not real. The box in front signals a physical degree of freedom that we can keep as such. The rest of the kinetic operator on the lefthand side must be treated by means of fakeons.

We write the Euclidean propagator as

$$\frac{1}{p_{\rm E}^2}-\frac{1}{M^2}F_\gamma(p_{\rm E}^2/M^2), \quad \text{where } F_\gamma(z)=\frac{z^{\gamma-1}}{1+z^\gamma}. \tag{4.2}$$

In the direct fakeon approach, we continue the Euclidean correlation functions to Minkowski spacetime as follows: all the thresholds, cuts, poles, etc., that depend on the fractional sector encoded in F_γ are treated by means of the average continuation, while those that are independent of the fractional sector are treated by means of the $i\epsilon$ prescription. If γ is a free parameter, the former can be distinguished from the latter because they are γ dependent.

In the case of the free propagator, we just need to apply the average continuation to the function F_γ and use the Feynman prescription for the physical pole. We get

$$\begin{aligned} G_1(p^2) &= \frac{i}{p^2+i\epsilon}+\frac{i}{M^2}{\rm Re}[F_\gamma(-p^2/M^2-i\epsilon)] \\ &= \frac{i}{p^2+i\epsilon}+\frac{i\theta(-p^2)(-p^2)^{\gamma-1}}{M^{2\gamma}+(-p^2)^\gamma} \\ &\quad +\frac{i\cos(\pi\gamma)\theta(p^2)(p^2)^{\gamma-1}}{M^{2\gamma}+(p^2)^\gamma}. \end{aligned} \tag{4.3}$$

The field equations of the theory with fakeons are then

$$\begin{aligned} \Box\phi &= \left.\frac{M^{2\gamma}}{M^{2\gamma}+\Box^\gamma}\right|_{\rm f} I_{\rm int} = i\Box G_1(-\Box)I_{\rm int} \\ &= \left[1-\frac{\theta(\Box)\Box^\gamma}{M^{2\gamma}+\Box^\gamma}+\frac{\cos(\pi\gamma)\theta(-\Box)(-\Box)^\gamma}{M^{2\gamma}+(-\Box)^\gamma}\right]I_{\rm int}. \end{aligned}$$

The decomposition approach is applied as follows. For $0<\gamma<1$, the function $F_\gamma(z)$ has no poles for $-\pi<{\rm Arg}[z]<\pi$ and a cut along the negative real axis. Using the Cauchy theorem, we can integrate along the cut and represent $F_\gamma(z)$ by means of the decomposition

$$F_\gamma(z)=\int_0^\infty\frac{\rho_\gamma(s){\rm d}s}{z+s}, \qquad \rho_\gamma(s)=\frac{1}{\pi}\frac{s^{\gamma-1}\sin(\pi\gamma)}{1+s^{2\gamma}+2s^\gamma\cos(\pi\gamma)}. \tag{4.4}$$

On the other hand, if

$$2k+1\leqslant\gamma<2k+3, \qquad k\in\mathbb{N},$$

the function $F_\gamma(z)$ has poles at $z=e^{\frac{i\pi}{\gamma}n}$, where n is any odd integer between $-2k-1$ and $2k+1$. Then

$$F_\gamma(z)=\int_0^\infty{\rm d}s\frac{\rho_\gamma(s)}{z+s}+R_\gamma(z), \quad R_\gamma(z)\equiv\frac{1}{\gamma}\sum_{\substack{n=-2k-1\\ n={\rm odd}^*}}^{2k+1}\frac{1}{z-e^{i\pi n/\gamma}}, \tag{4.5}$$

where the star on "odd" means that when γ itself is odd ($\gamma=2k+1$), the contribution of $n=-2k-1$ is ignored; otherwise, the pole $1/(z+1)$ is counted twice. It is easy to check (4.5) in simple cases such as $\gamma\in\mathbb{N}_+$, $\gamma=1/2$, $1/4$, $2/3\ldots$, etc.

Diagrams are built as explained previously, using (4.5) and applying the fakeon diagrammatics at fixed s and n. The pole at $p^2=0$ is treated by means of the $i\epsilon$ prescription, while the poles at $-z=p^2=M^2s$ and those at $-z=p^2=-M^2e^{i\pi n/\gamma}$ are treated as fakeons. The sum over n and the integral over s are done at the end. Note that there are no tachyons (for which the fakeon prescription is not guaranteed to work).

In particular, the propagator (4.3) is also equal to

$$\begin{aligned} G_1(p^2) &= \frac{i}{p^2+i\epsilon}-\mathcal{P}\int_0^\infty{\rm d}s\frac{i\rho_\gamma(s)}{p^2-sM^2}, \\ G_1(p^2) &= \frac{i}{p^2+i\epsilon}-\mathcal{P}\int_0^\infty{\rm d}s\frac{i\rho_\gamma(s)}{p^2-sM^2} \\ &\quad -\frac{1}{\gamma}\mathcal{P}\sum_{\substack{n=-2k-1\\ n={\rm odd}^*}}^{2k+1}\frac{i}{p^2+M^2e^{i\pi n/\gamma}}, \end{aligned} \tag{4.6}$$

for $0<\gamma<1$ and $2k+1\leqslant\gamma<2k+3$, $k\in\mathbb{N}$, respectively.

B. Model 2

In the $\mathcal{L}_2$ case, the classical field equations

$$\Box\left(1+\left(\frac{\Box^2}{M^4}\right)^{\gamma/2}\right)\phi = I_{\rm int} \tag{4.7}$$

are acceptable in the form they appear.

We write the Euclidean propagator as

$$\frac{1}{p_{\rm E}^2}\frac{1}{\left(1+\frac{(p_{\rm E}^2)^2}{M^4}\right)^{\gamma/2}}=\frac{1}{p_{\rm E}^2}-\frac{p_{\rm E}^2}{M^4}F_{\gamma/2}(u)=\frac{1}{p_{\rm E}^2}[1-uF_{\gamma/2}(u)], \tag{4.8}$$

where $u=(p_{\rm E}^2)^2/M^4$ and $F_{\gamma/2}(u)$ can be read from (4.2).

Again, we treat the pole at $p_{\rm E}^2=-p^2=0$ as physical by means of the Feynman $i\epsilon$ prescription and the remnant by

means of the fakeon approach at fixed s and n, using the decomposition (4.5).

For $0 < \gamma < 2$, the Minkowskian propagator is

$$G_2(p^2) = \frac{i}{p^2 + i\epsilon} - \int_0^\infty \mathrm{d}s \frac{ip^2\rho_{\gamma/2}(s)}{(p^2)^2 + sM^4}, \quad (4.9)$$

while for $4k + 2 \leqslant \gamma < 4k + 6$, $k \in \mathbb{N}$, it is

$$G_2(p^2) = \frac{i}{p^2 + i\epsilon} - \int_0^\infty \mathrm{d}s \frac{ip^2\rho_{\gamma/2}(s)}{(p^2)^2 + sM^4} - \frac{2}{\gamma} \sum_{\substack{n=-2k-1 \\ n=\mathrm{odd}^*}}^{2k+1} \frac{ip^2}{(p^2)^2 - M^4 \mathrm{e}^{2i\pi n/\gamma}}, \quad (4.10)$$

where, as before, n is any odd integer number between $-2k - 1$ and $2k + 1$. There is a continuum of fakeon poles at $p^2 = \pm iM^2\sqrt{s}$ and a discrete set of fakeon poles at $p^2 = \pm M^2 \mathrm{e}^{i\pi n/\gamma}$. They all come in complex conjugate pairs.

A few examples may help. In the case $\gamma = 1$, we have

$$F_{1/2}(u) = \frac{1}{\sqrt{u} + u} = \int_0^\infty \frac{\mathrm{d}s}{\pi\sqrt{s}(1 + s)} \frac{1}{s + u},$$

while $\gamma = 1/2$ gives

$$F_{1/4}(u) = \frac{1}{u^{3/4} + u} = \int_0^\infty \frac{\mathrm{d}s}{\sqrt{2}\pi s^{3/4}(1 + \sqrt{2}s^{1/4} + \sqrt{s})} \frac{1}{s + u}.$$

A simple situation where the decomposition with discrete fakeons can be checked straightforwardly is the case $\gamma = 3$, which gives

$$F_{3/2}(u) = \frac{\sqrt{u}}{1 + u^{3/2}} = f_{3/2}(u) + R_{3/2}(u), \qquad R_{3/2}(u) = \frac{2}{3} \frac{1 + 2u}{1 + u + u^2},$$
$$f_{3/2}(u) = \int_0^\infty \mathrm{d}s \frac{\rho_{3/2}(s)}{s + u} = -\frac{2 + \sqrt{u}}{3(1 + \sqrt{u})(1 + \sqrt{u} + u)}.$$

The expression (4.10) can be used inside loop diagrams. A loop integral is first evaluated at fixed s and n in the Euclidean framework. Then one performs the average continuation to Minkowski spacetime, still at fixed s and n. Finally, one integrates over s and sums on n.

For every s and n, the loop integrals have the usual structure, the integrands being ratios of polynomials of the momenta. It is also straightforward to use the diagrammatic rules of [20,21].

More general models can be studied along the same lines.

C. Other formulations

As said, the options are infinitely many and lead to inequivalent theories. An alternative decomposition for Model 2 is studied in Ref. [28]. The main difference is that our choice preserves the oddity of (4.8) under $z = p_{\mathrm{E}}^2 \to -z$, while the arrangement of [28] breaks the propagator into the sum of the physical pole plus an even function of p^2.

Moreover, in the spirit of Sec. II, we point out an infinite class of decompositions aligned with our choice (4.8), which are

$$F_{\gamma/2}(u) = \frac{(u^n)^{(\gamma-2)/(2n)}}{1 + (u^n)^{\gamma/(2n)}} = \int_0^\infty \mathrm{d}s \frac{\rho_n(s)}{u^n + s}, \qquad u > 0,$$
$$\rho_n(s) = \frac{s^{(\gamma-2)/(2n)}}{\pi} \frac{s^{\gamma/(2n)} \sin(\pi/n) - \sin(\pi(\gamma - 2)/(2n))}{1 + s^{\gamma/n} + 2s^{\gamma/(2n)} \cos(\pi\gamma/(2n))},$$

for $0 < \gamma < 2n$. For the other values of γ we need to add discrete sets of fakeons as before.

V. FRACTIONAL COVARIANT D'ALEMBERTIANS

In this section, we extend the formulations to fractional powers of covariant d'Alembertians. We focus on gauge theories, since gravity can be treated similarly.

Consider the Lagrangians

$$\mathcal{L}_1 = -\bar{\phi} D_\mu D^\mu \left(1 + \frac{(D_\nu D^\nu)^\gamma}{M^{2\gamma}}\right)\phi + \mathcal{L}_{\mathrm{int}},$$
$$\mathcal{L}_2 = -\bar{\phi} D_\mu D^\mu \left(1 + \left(\frac{(D_\nu D^\nu)^2}{M^4}\right)^{\gamma/2}\right)\phi + \mathcal{L}_{\mathrm{int}},$$

where $D_\mu = \partial_\mu - ieA_\mu$ is the covariant derivative.

Below, we derive the vertices and explain how to build the correlation functions. We summarize here the rules: *a*) in the direct approach to Model 1, we switch $\mathcal{L}_1$ to the Euclidean framework, then switch the correlation functions back to Minkowski spacetime by means of the average continuation; *b*) in the decomposition approach (for both $\mathcal{L}_1$ and $\mathcal{L}_2$), we also switch the Lagrangian to the Euclidean framework, write the correlation functions by means the appropriate density $\rho(s)$ (with the possible addition of discrete sets of fakeons, labeled by some integer n), average-continue the Euclidean loop integrals

to Minkowski spacetime at fixed s and n, and finally integrate over s and sum over n.

A. Vertices

The densities can also be used as efficient tools to derive the vertices. We first work in Model 2, then in Model 1. For definiteness, we assume $0 < \gamma < 2$ for Model 2 and $0 < \gamma < 1$ for Model 1. In the other cases, we have to include discrete sets of fakeons.

The scalar propagator (4.9) leads to the covariantized expression

$$-\frac{i}{D_\mu D^\mu - i\epsilon} + iD_\nu D^\nu \int_0^\infty \frac{\rho_{\gamma/2}(s)\mathrm{d}s}{(D_\mu D^\mu)^2 + sM^4}, \qquad (5.1)$$

where $\rho_{\gamma/2}(s)$ is the one of (4.4), which can be expanded in powers of the coupling as follows. Focusing on the integral in the last term of (5.1) and writing

$$(D_\mu D^\mu)^2 \equiv \Box^2 + \Upsilon,$$
$$\Upsilon = V_{\mu\nu\rho}\partial^\mu\partial^\nu\partial^\rho + V_{\mu\nu}\partial^\mu\partial^\nu + V_\mu\partial^\mu + V,$$

for some functions $V_{\mu\nu\rho}$, $V_{\mu\nu}$, V_μ, and V, the geometric series gives

$$\int_0^\infty \frac{\rho_{\gamma/2}(s)\mathrm{d}s}{\Box^2 + sM^4 + \Upsilon} = \sum_{m=0}^\infty \int_0^\infty \frac{\rho_{\gamma/2}(s)\mathrm{d}s}{\Box^2 + sM^4}\left(-\Upsilon\frac{1}{\Box^2 + sM^4}\right)^m. \qquad (5.2)$$

At this point, we define

$$F_{x_1,\dots,x_{m+1}} \equiv \int_0^\infty \frac{(-1)^m \rho_{\gamma/2}(s)\mathrm{d}s}{\prod_{i=1}^{m+1}(x_i + sM^4)}, \qquad m \in \mathbb{N}, \qquad (5.3)$$

and switch to momentum space. The Fourier transform of (5.2) with momentum p is

$$\int \mathrm{d}^4x \int_0^\infty \frac{\rho_{\gamma/2}(s)\mathrm{d}s}{\Box^2 + sM^4 + \Upsilon}\mathrm{e}^{ip\cdot x} = \sum_{m=0}^\infty \int \tilde\Upsilon(k_1)\cdots\tilde\Upsilon(k_m) F_{((p-\hat k_m)^2)^2,\cdots((p-\hat k_1)^2)^2,(p^2)^2}, \qquad (5.4)$$

where $\hat k_j = k_1 + \cdots + k_j$, while k_i are the incoming momenta of the $\tilde\Upsilon$ insertions (Fourier transforms of Υ). The k_i-integration measures are understood.

Formula (5.4) shows both a compact expression (to the right) and a decomposed expression (to the left). Compact expressions of this type can be used in the direct approach to Model 1.

In the case of Model 1, we write

$$D_\mu D^\mu \equiv \Box + \Xi, \qquad \Xi = -2ieA_\mu\partial^\mu - ie(\partial^\mu A_\mu) - e^2 A_\mu A^\mu.$$

The geometric series gives

$$\int \mathrm{d}^4x \int_0^\infty \frac{\rho_\gamma(s)\mathrm{d}s}{\Box + s + \Xi - i\epsilon}\mathrm{e}^{ip\cdot x} = \sum_{m=0}^\infty \int \tilde\Xi(k_1)\cdots\tilde\Xi(k_m) H_{-(p-\hat k_m)^2 - i\epsilon,\cdots -(p-\hat k_1)^2 - i\epsilon, -p^2 - i\epsilon}, \qquad (5.5)$$

where H is F with $\rho_{\gamma/2}(s) \to \rho_\gamma(s)$ and $M \to 1$. Then we apply the average continuation at fixed s.

B. Gauge invariance

Now, we illustrate how gauge invariance works at the level of correlations functions, through the Ward-Takahashi-Slavnov-Taylor (WTST) identities [37].

To keep formulas simple, we consider fractional scalar QED models with Lagrangian

$$\mathcal{L}_1 = -\frac{1}{4}F_{\mu\nu}F^{\mu\nu} - \bar\varphi(D^\mu D_\mu)^\gamma\varphi,$$
$$\mathcal{L}_2 = -\frac{1}{4}F_{\mu\nu}F^{\mu\nu} - \bar\varphi[(D^\mu D_\mu)^2]^{\gamma/2}\varphi, \qquad (5.6)$$

where φ is a charged scalar field. The theories (5.6) are invariant under the infinitesimal gauge transformation $\delta\varphi = ie\Lambda\varphi$, $\delta A_\mu = \partial_\mu\Lambda$.

C. WTST identities: direct approach

When needed, the switch to Euclidean space is understood. We comment on the gauge invariance of the average continuation to Minkowski spacetime at the end.

We begin with the direct approach to Model 1, where we can apply compact formulas. Using the density of (2.8), the first order of (5.5) in $\tilde\Xi$ gives

$$\tilde\Xi(k)H_{-(p-k)^2 - i\epsilon, -p^2 - i\epsilon} = \tilde\Xi(k)\frac{[-(p-k)^2 - i\epsilon]^{-\gamma} - (-p^2 - i\epsilon)^{-\gamma}}{-(p-k)^2 + p^2}. \qquad (5.7)$$

Next, writing

$$D_\mu D^\mu = \Box + \Xi = -p^2 + eA_\mu(k)(2p_\mu - k_\mu) + \mathcal{O}(A^2)$$

and acting on $\mathrm{e}^{ip\cdot x}$, we find that the vertex with one gauge field is

$$\tilde\Xi(k)H_{-(p-k)^2 - i\epsilon, -p^2 - i\epsilon} = eA_\mu(k)U^\mu$$

with

$$U^\mu = -\int_0^\infty \frac{(2p^\mu - k^\mu)\rho_\gamma(s)\mathrm{d}s}{((p-k)^2 - s + i\epsilon)(p^2 - s + i\epsilon)} = (2p^\mu - k^\mu)\frac{[-(p-k)^2 - i\epsilon]^{-\gamma} - (-p^2 - i\epsilon)^{-\gamma}}{-(p-k)^2 + p^2}. \tag{5.8}$$

The generalization of the usual Ward identity is obtained by replacing $A^\mu(k)$ with $-ik^\mu$. Using the right expression of (5.8), we find

$$-ik^\mu U_\mu = -\frac{i}{[-(p-k)^2 - i\epsilon]^\gamma} + \frac{i}{(-p^2 - i\epsilon)^\gamma}. \tag{5.9}$$

If we move to Euclidean space, this formula gives the basic Euclidean Ward identity. Indeed, the righthand side turns into the difference between two Euclidean propagators with the expected momenta. This proves that the Euclidean correlation functions are gauge-invariant.

Moreover, the analytic continuation is a gauge-invariant operation (on gauge-invariant Euclidean correlation functions), because the WTST identities, such as (5.9), hold at the integrand level. During the continuation, the identities continue to hold simply because they are "identities", hence the same operations act on their lefthand sides as on their righthand sides. They also hold during the average continuation, because it is an average of analytic continuations.

For example, when we average the $i\epsilon$ contributions (5.9) with its $-i\epsilon$ counterpart, the righthand side gives the difference between two propagators of Model 1 with the correct momenta, while the average of U_μ gives the vertex of Model 1.

D. WTST identities: decomposition approach

As said, the key property of the WTST identities is that they can be proved at the level of integrands, without the need to calculate any diagrams. In the decomposition approach, they hold at fixed s and n, where they look like the WTST identities of ordinary theories.

Specifically, using the mid expression of (5.8), we easily find

$$-ik_\mu(k)U^\mu = -i[(p-k)^2 - p^2]\int_0^\infty \frac{\rho_\gamma(s)\mathrm{d}s}{((p-k)^2 - s + i\epsilon)(p^2 - s + i\epsilon)} = \int_0^\infty \frac{i\rho_\gamma(s)\mathrm{d}s}{(p-k)^2 - s + i\epsilon} - \int_0^\infty \frac{i\rho_\gamma(s)\mathrm{d}s}{p^2 - s + i\epsilon}.$$

The second expression is the action on the decomposed vertices, while the third one is the difference of two decomposed propagators.

At the level of integrands, we just have the usual Ward identity

$$-ik_\mu \frac{i}{(p-k)^2 - s + i\epsilon}(2p_\mu - k_\mu)\frac{i}{p^2 - s + i\epsilon} = \frac{i}{(p+k)^2 - s + i\epsilon} - \frac{i}{p^2 - s + i\epsilon}.$$

One proceeds in a similar way in the case of Model 2.

VI. CLASSICIZATION AND DEGREES OF FREEDOM

In this section, we study the number of degrees of freedom of fractional theories. In the classical limit, we have two sources of nonlocality: the fractional power of derivative operators and fakeons. This raises the concern that an infinite number of initial conditions may be needed to uniquely determine the solution of the field equations. We prove that it is not so. Actually, only the expected, physical degrees of freedom propagate.

In nonfractional theories, the issue was studied in Ref. [38], where it was shown that fakeons are immune from the problem just stated. In fractional models, we must investigate the impact of the additional nonlocality due to the fractional power.

We illustrate the procedure in simple solvable examples. We assume that γ is truly fractional, i.e., $\gamma = m/n$ with $m, n \in \mathbb{N}$, $n \neq 0$, and concentrate on quantum mechanics ($D = 1$).

Since we are working in the realm of perturbative quantum field theory, it is sufficient to count the number of degrees of freedom when interactions are switched off. Interactions do not affect the counting, since they are turned on iteratively. We focus on models of the extended classes considered in Sec. IV, where the kinetic operator is nonsingular when the fractional power is turned off. The models of Sec. II are singular in this respect. It is not known at present how to properly count the number of degrees of freedom in cases like (2.1), relying on standard QFT techniques.

Consider equation (4.7) with a harmonic force:

$$\left(1 + \left(\frac{\mathrm{d}^4/\mathrm{d}t^4}{M^4}\right)^{\gamma/2}\right)\ddot{x} = -\omega^2 x. \tag{6.1}$$

The correct equation of motion of the theory with fakeons is obtained by inverting the operator between parentheses by means of the fakeon prescription (see, for example, [38]). We find

$$\ddot{x}(t) = -\omega^2 \int_{-\infty}^{+\infty} \mathrm{d}t' G_{\mathrm{f}}^{\gamma}(t-t')x(t'),$$
$$G_{\mathrm{f}}^{\gamma}(t) = \int_{-\infty}^{+\infty} \frac{\mathrm{d}\varpi}{2\pi} \frac{M^{2\gamma}\mathrm{e}^{-i\varpi t}}{M^{2\gamma}+(\varpi^2)^{\gamma}}, \tag{6.2}$$

where $G_{\mathrm{f}}^{\gamma}(t)$ denotes the fakeon Green function. For the uses below, we need its asymptotic behavior for $0<\gamma<1/2$, which is

$$G_{\mathrm{f}}^{\gamma}(t) \simeq \frac{\sin(\pi\gamma)\Gamma(1+2\gamma)}{\pi M^{2\gamma}|t|^{1+2\gamma}}, \tag{6.3}$$

and

$$G_{\mathrm{f}}^{1}(t) = \frac{M}{2}\mathrm{e}^{-M|t|}. \tag{6.4}$$

Switching to Fourier transforms, we search for solutions to (6.1) of the form

$$x(t) = \sum_j c_j \mathrm{e}^{i\lambda_j t M}, \tag{6.5}$$

where c_j are arbitrary coefficients. The frequencies λ_j solve the equation

$$[1+(\lambda_j^4)^{\gamma/2}]\lambda_j^2 = \tilde{\omega}^2, \tag{6.6}$$

where $\tilde{\omega}=\omega/M$. Squaring and then raising to the power m, we obtain the polynomial equations

$$(1+v_j)^{2m}v_j^{2n} = \tilde{\omega}^{4m}, \tag{6.7}$$

for the quantities $v_j=(\lambda_j^4)^{\gamma/2}$. This is already enough to prove that the number of degrees of freedom is finite, since (6.7) admits a finite number of solutions.

The right solutions λ_j are those that solve (6.2) as well. In particular, the integral expressing $\ddot{x}(t)$ must be convergent. Moreover, we know from Appendix A that the quantities v_j must satisfy the inequality $|\mathrm{Arg}[v_j]| \leqslant \pi\gamma/2$.

Now we prove that the acceptable λ_j are the physical ones, which are those that match the perturbative expansion of (6.2): $\lambda_j \simeq \pm\tilde{\omega} + \mathcal{O}(\tilde{\omega}^2)$.

The first example we consider is the borderline case $m=1$, $n=1$, $\gamma=1$, which provides a way to treat the kinetic operator $\Box(1+\sqrt{\Box^2/M^2})$. This is interesting because it contains the "absolute value $|\Box|$ of box" (in the form $\sqrt{\Box^2}$). We have $v_j=\sqrt{\lambda_j^4}$, so the inequality $|\mathrm{Arg}[(z^4)^{\gamma/2}]| \leqslant \pi\gamma/2$ implies $\mathrm{Re}[v_j] \geqslant 0$.

The v_j equation (6.7) has a positive solution, which is

$$\nu^* = \frac{1}{2}\left(\sqrt{1+4\tilde{\omega}^2}-1\right),$$

and three solutions with negative real parts, which must be discarded. Inverting $\nu^*=\sqrt{\lambda_j^4}$ by means of (A2), we find the four results $\lambda_j=(1,-i,i,-1)\sqrt{\nu^*}$. When $\nu^* \geqslant 1$ only the first and last options are acceptable since the other two make the convolution of (6.2) divergent, by (6.4). However, when $\nu^*<1$, all four make the convolution convergent, which is a source of concern since the physical solutions are only two.

This caveat was explained in Ref. [38], where was shown that it is not convenient to impose the fakeon prescription for special values of the parameters (such as $\gamma=1$ here). Rather, the situation of interest must be reached as a limit from a generic deformation. This means that we need to work with an arbitrary, fractional $\gamma=m/n$, show that the degrees of freedom are the physical ones there (which we do below), and take the limit $\gamma\to 1^-$ at the end. In so doing, it becomes visible that $\gamma=1$ only inherits the physical degrees of freedom.

The second example we consider is the case $m=1$, $n=2$, $\gamma=1/2$. Now, $v_j=(\lambda_j^4)^{1/4}$ and the v_j equation

$$(1+v_j)^2 v_j^4 = \tilde{\omega}^4$$

has a unique acceptable solution, which is

$$\nu^* = \frac{1}{3}\left(a+\frac{1}{a}-1\right),$$
$$a = 2^{-1/3}\left(3\tilde{\omega}\sqrt{81\tilde{\omega}^2-12}+18\tilde{\omega}-2\right)^{1/3},$$

since the other five have $|\mathrm{Arg}[v_j]|>\pi/4$. Note that ν^* is real. Inverting (A3), we find $\lambda_j=(1,-i,i,-1)\nu^*$, but only the first and last ones are acceptable, since by (6.3), the other two make the convolution of (6.2) divergent.

The third example we treat is the case $m=1$, $n=4$, $\gamma=1/4$. Now, $v_j=(\lambda_j^4)^{1/8}$, and the v_j equation

$$(1+v_j)^2 v_j^8 = \tilde{\omega}^4,$$

is solved by a unique real solution ν^*. The other seven solutions violate the condition $|\mathrm{Arg}[(z^4)^{\gamma/2}]| \leqslant \pi\gamma/2$. Inverting (A3), we find $\lambda_j=(1,-i,i,-1)(\nu^*)^2$, and again only $\lambda_j=\pm(\nu^*)^2$ are acceptable, since the others make the convolution of (6.2) divergent, by (6.3).

Now we treat the general case for $\tilde{\omega}$ small. The solutions of (6.7) read

$$v_j \simeq -1+\cdots, \qquad v_j \simeq \tilde{\omega}^{2m/n}\mathrm{e}^{\pi i q/n}+\cdots,$$

where q is an integer. The first class of solutions is not acceptable because they have a negative real part. As far as the second class is concerned, the condition $|\mathrm{Arg}[v_j]| \leqslant \pi\gamma/2$ implies $|q| \leqslant m/2$.

Now we have to solve

$$(\lambda_j^4)^{m/(2n)} \simeq \tilde{\omega}^{2m/n} \mathrm{e}^{\pi i q/n} + \cdots .$$

Raising by $2n/m$, the phase satisfies $|\pi q/n \cdot 2n/m| = |2\pi q/m| \leqslant \pi$, and the fourth root gives

$$\lambda_j \simeq (1, i, -i, -1)\tilde{\omega} \mathrm{e}^{\pi i q/(2m)} + \cdots .$$

All such solutions have nonvanishing imaginary parts and make the convolution of (6.2) divergent, except for

$$\lambda_j \simeq (1, -1)\tilde{\omega} + \cdots .$$

Thus, only these two solutions are acceptable, at least perturbatively in $\tilde{\omega}$. They are the expected, physical ones.

To conclude, the nonlocal structure of the equations does not burden (6.2) with the need to fix other initial conditions besides the physically expected ones, which are associated with the pole $p^2 = 0$ of propagators such as (4.10).

VII. CONCLUSIONS

Quantum field theories with fractional or continuous powers of the d'Alembert operator represent a challenging arena to extend knowledge about QFT beyond its standard enclosure.

A well-defined classical limit with a finite number of initial conditions is not guaranteed, because the field equations are nonlocal and generically nonreal or non-Hermitian. At the quantum level, on the other hand, one must pay attention to perturbative unitarity. Fakeons provide a simple way to formulate unitary fractional models with an appropriate classical limit and the right set of degrees of freedom.

The simplest formulation is the "direct" one. It amounts to continuing the correlation functions from Euclidean space to Minkowski spacetime using the fakeon approach for the fractional part of the power. However, this is not the only way to employ fakeons for fractional theories. We have shown that infinitely many alternatives are available, and they are all inequivalent, in the sense that they generate different correlation functions. In most cases, this is visible already at the tree level. We also demonstrated it in bubble diagrams.

Finally, we have coupled fractional theories to gauge fields and gravity, preserving the Ward and Cutkosky identities in all formulations.

Fractional models may or may not be useful to describe the physics of fundamental interactions. However, in many cases they may describe systems approximately as effective field theories. Potential applications range from statistical systems to critical and off-critical phenomena, and more generally descriptions of systems where certain effects of the experimental apparatus or the boundary conditions drive the physics off-shell.

ACKNOWLEDGMENTS

The author is grateful to F. Briscese and G. Calcagni for useful discussions.

DATA AVAILABILITY

There are no publicly available research data or software supporting this manuscript. Requests for further information or data should be sent to the author.

APPENDIX A: FRACTIONAL POWERS

In this Appendix, we give details on the functions z^γ and $(z^2)^{\gamma/2}$, $z \in \mathbb{C}$, used in this paper. The function z^γ is defined by the standard cut on the negative real axis $z \leqslant 0$. Then it follows that $(z^2)^{\gamma/2}$ has a cut in $\mathrm{Re}[z] = 0$, which divides the complex plane into two disjoint regions.

There are two options to define z^γ on the real axis $z = x \in \mathbb{R}$: $(x + i\epsilon)^\gamma$ and $(x - i\epsilon)^\gamma$, where $\epsilon \to 0^+$. Both have nonvanishing imaginary parts for $x < 0$, which makes the field equations (2.2) not acceptable.

On the other hand, we can understand the function $(z^2)^{\gamma/2}$ as $(x + i\epsilon)^{\gamma/2}(x - i\epsilon)^{\gamma/2}$ for $z = x \in \mathbb{R}$. If we write this expression as $(x^2 + \epsilon^2)^{\gamma/2}$, the parameter ϵ becomes irrelevant, and hence we obtain $(x^2)^{\gamma/2}$, which is real on the whole real axis. This makes the field equations (2.3) acceptable (Model 2).

Writing $z = \rho \mathrm{e}^{i\theta}$ on the complex plane, we have

$$(z^2)^{\gamma/2} = \begin{cases} \rho^\gamma \mathrm{e}^{i\theta\gamma} & \text{for } -\frac{\pi}{2} < \theta < \frac{\pi}{2}, \\ \rho^\gamma \mathrm{e}^{i(\theta-\pi)\gamma} & \text{for } \frac{\pi}{2} < \theta \leqslant \pi, \\ \rho^\gamma \mathrm{e}^{i(\theta+\pi)\gamma} & \text{for } -\pi \leqslant \theta < -\frac{\pi}{2}. \end{cases} \tag{A1}$$

For example, $\sqrt{z^2} = z$ for $\mathrm{Re}[z] > 0$ and $\sqrt{z^2} = -z$ for $\mathrm{Re}[z] < 0$. In all cases, $\mathrm{Re}[\sqrt{z^2}] \geqslant 0$. Moreover, $|\mathrm{Arg}[(z^2)^{\gamma/2}]| \leqslant \pi\gamma/2$. In particular, $\mathrm{Re}[(z^2)^{\gamma/2}] \geqslant 0$ for every $\gamma \leqslant 1$.

Formula (A1) decomposes $(z^2)^{\gamma/2}$ in terms of its modulus and argument, assuming the principal branch for fractional powers. The condition on the argument is a consequence of first squaring z and then taking the square root of z^2.

We also have

$$\sqrt{z^4} = \begin{cases} z^2 & \text{for } |\theta| < \frac{\pi}{4} \text{ and } \frac{3\pi}{4} < |\theta| \leqslant \pi, \\ -z^2 & \text{for } \frac{\pi}{4} < |\theta| < \frac{3\pi}{4}, \end{cases} \qquad \mathrm{Re}[(z^4)^{1/2}] \geqslant 0. \tag{A2}$$

with cuts on the diagonals of the complex plane. It is straightforward to obtain (with the same cuts)

$$(z^4)^{\gamma/2} = \begin{cases} \rho^{2\gamma} e^{2\theta\gamma i} & \text{for } -\frac{\pi}{4} < \theta < \frac{\pi}{4} \\ \rho^{2\gamma} e^{(2\theta-\pi)\gamma i} & \text{for } \frac{\pi}{4} < \theta < \frac{3\pi}{4}, \\ \rho^{2\gamma} e^{2(\theta-\pi)\gamma i} & \text{for } \frac{3\pi}{4} < \theta \leqslant \pi, \\ \rho^{2\gamma} e^{(2\theta+\pi)\gamma i} & \text{for } -\frac{3\pi}{4} < \theta < -\frac{\pi}{4}, \\ \rho^{2\gamma} e^{2(\theta+\pi)\gamma i} & \text{for } -\pi \leqslant \theta < -\frac{3\pi}{4}, \end{cases} \tag{A3}$$

As before, $|\mathrm{Arg}[(z^4)^{\gamma/2}]| \leqslant \pi\gamma/2$.

APPENDIX B: ANALYTIC CONTINUATION OF THE BUBBLE DIAGRAM

In this Appendix, we derive the analytic continuation (3.14) more explicitly. For $\mathrm{Re}[z] > 0$, the integral (3.12) evaluates to

$$f(z,s,\sigma) = \frac{i}{\sqrt{(s+\sigma+iz)^2 - 4iz\sigma}} \ln \frac{s-\sigma+iz+\sqrt{(s+\sigma+iz)^2-4iz\sigma}}{s-\sigma+iz-\sqrt{(s+\sigma+iz)^2-4iz\sigma}} + \text{c.c.},$$

It is easy to check that the function $f(z,s,\sigma)$ is analytic when the arguments of the square roots become real and negative. Instead, it has a cut for imaginary z, where the logarithm tends to $-i\pi$ from $\mathrm{Re}[z] > 0$. When the imaginary axis is crossed from $\mathrm{Re}[z] > 0$ to $\mathrm{Re}[z] < 0$, the analytic continuation gives an extra contribution obtained by replacing the logarithm with $2\pi i$. The result

$$f^{\mathrm{an}}(z,s,\sigma) = -f(-z,s,\sigma) + \frac{2\pi}{\sqrt{(s+\sigma+iz)^2-4iz\sigma}} + \frac{2\pi}{\sqrt{(s+\sigma-iz)^2+4iz\sigma}}$$

for $\mathrm{Re}[z] < 0$, matches the one of (3.14), having used (3.13).

As far as the function (3.16) is concerned, we find

$$g(z,s,\sigma) = \frac{i}{\sqrt{(s-\sigma+iz)^2+4iz\sigma}} \ln \frac{s+\sigma+iz+\sqrt{(s-\sigma+iz)^2+4iz\sigma}}{s+\sigma+iz-\sqrt{(s-\sigma+iz)^2+4iz\sigma}} + \text{c.c.}$$

for $\mathrm{Re}[z] > 0$ and $g^{\mathrm{an}}(z,s,\sigma) = -g(-z,s,\sigma)$ for $\mathrm{Re}[z] < 0$.

[1] A. Pais and G. E. Uhlenbeck, On field theories with non-localized action, Phys. Rev. **79**, 145 (1950).

[2] G. V. Efimov, Non-local quantum theory of the scalar field, Commun. Math. Phys. **5**, 42 (1967); G. V. Efimov, Quantization of non-local field theory, Int. J. Theor. Phys. **10**, 19 (1974); G. V. Efimov, *Nonlocal Interactions of Quantized Fields* (Nauka, Moscow, 1977).

[3] N. V. Krasnikov, Nonlocal gauge theories, Teor. Mat. Fiz. **73**, 235 (1987)) [Theor. Math. Phys. **73**, 1184 (1987].

[4] Yu. V. Kuz'min, The convergent nonlocal gravitation, Yad. Fiz. **50**, 1630 (1989) [Sov. J. Nucl. Phys. **50**, 1011 (1989)].

[5] E. T. Tomboulis, Super-renormalizable gauge and gravitational theories, arXiv:hep-th/9702146.

[6] L. Modesto, Super-renormalizable quantum gravity, Phys. Rev. D **86**, 044005 (2012), arXiv:1107.2403.L. Modesto, Finite quantum gravity, arXiv:1305.6741; F. Briscese, L. Modesto, and S. Tsujikawa, Super-renormalizable or finite completion of the Starobinsky theory, Phys. Rev. D **89**, 024029 (2014), arXiv:1308.1413; L. Modesto and L. Rachwał, Universally finite gravitational and gauge theories, Nucl. Phys. **B900**, 147 (2015), arXiv:1503.00261; L. Modesto and L. Rachwał, Super-renormalizable and finite gravitational theories, Nucl. Phys. **B889**, 228 (2014), arXiv:1407.8036; L. Modesto, Multidimensional finite quantum gravity, arXiv:1402.6795; G. Calcagni, B. L. Giacchini, L. Modesto, T. de Paula Netto, and L. Rachwał, Renormalizability of nonlocal quantum gravity coupled to matter, J. High Energy Phys. 09 (2023) 034.

[7] E. Marcus, Higher-derivative gauge and gravitational theories, Ph.D. thesis, University of California, Los Angeles, 1998.

[8] S. Lanza, Renormalizability and finiteness of nonlocal quantum gravity, etd-06202016-152710, Laurea thesis at Pisa University.

[9] V. A. Alebastrov and G. V. Efimov, A proof of the unitarity of S-matrix in a nonlocal quantum field theory, Commun. Math. Phys. **31**, 1 (1973).

[10] F. Briscese and L. Modesto, Cutkosky rules and perturbative unitarity in Euclidean nonlocal quantum field theories, Phys. Rev. D **99**, 104043 (2019).

[11] T. Biswas, E. Gerwick, T. Koivisto, and A. Mazumdar, Towards singularity and ghost free theories of gravity, Phys. Rev. Lett. **108**, 031101 (2012); T. Biswas, A. Conroy, A. S. Koshelev, and A. Mazumdar, Generalized ghost-free quadratic curvature gravity, Classical Quantum Gravity **31**, 015022 (2014); L. Buoninfante, A. S. Koshelev, G. Lambiase, and A. Mazumdar, Classical properties of nonlocal, ghost- and singularity-free gravity, J. Cosmol. Astropart. Phys. 09 (2018) 034.A. S. Koshelev and A. Tokareva, Unitarity of Minkowski nonlocal theories made explicit, Phys. Rev. D **104**, 025016 (2021); F. Briscese, G. Calcagni, L. Modesto, and G. Nardelli, Form factors, spectral and Källén-Lehmann representation in nonlocal quantum gravity, J. High Energy Phys. 08 (2024) 204.

[12] T. D. Lee and G. C. Wick, Negative metric and the unitarity of the S-matrix, Nucl. Phys. **B9**, 209 (1969); T. D. Lee and G. C. Wick, Finite theory of quantum electrodynamics, Phys. Rev. D **2**, 1033 (1970); R. E. Cutkosky, P.V Landshoff, D. I. Olive, and J. C. Polkinghorne, A non-analytic S matrix, Nucl. Phys. **B12**, 281 (1969); T. D. Lee, A relativistic complex pole model with indefinite metric, in *Quanta: Essays in Theoretical Physics Dedicated to Gregor Wentzel* (Chicago University Press, Chicago, 1970), p. 260; N. Nakanishi, Lorentz noninvariance of the complex-ghost relativistic field theory, Phys. Rev. D **3**, 811 (1971); B. Grinstein, D. O'Connell, and M. B. Wise, Causality as an emergent macroscopic phenomenon: The Lee-Wick O(N) model, Phys. Rev. D **79**, 105019 (2009).

[13] M. J. G. Veltman, Unitarity and causality in a renormalizable field theory with unstable particles, Physica **29**, 186 (1963); H. Yamamoto, Convergent field theory with complex masses, Prog. Theor. Phys. **42**, 707 (1969); H. Yamamoto, Quantum field theory of complex mass, Prog. Theor. Phys. **44**, 272 (1970); N. Nakanishi, Indefinite metric quantum field theory, Prog. Theor. Phys. Suppl. **51**, 1 (1972); P. D. Mannheim, Unitarity of loop diagrams for the ghostlike $1/(k^2 - M_1^2) - 1/(k^2 - M_2^2)$ propagator, Phys. Rev. D **98**, 045014 (2018); L. Buoninfante, Remarks on ghost resonances, J. High Energy Phys. 02 (2025) 186; J. Liu, L. Modesto, and G. Calcagni, Quantum field theory with ghost pairs, J. High Energy Phys. 02 (2023) 140; A. Tokareva, Background-induced complex mass states of graviton: Quantization and tensor power spectrum, arXiv:2405.09527; M. Asorey, G. Krein, and I. L. Shapiro, Normal bound states out of massive complex ghosts degrees of freedom in superrenormalizable quantum gravity theories, J. High Energy Phys. 01 (2025) 113.

[14] B. Holdom and J. Ren, QCD analogy for quantum gravity, Phys. Rev. D **93**, 124030 (2016); G. P. de Brito, Quadratic gravity in analogy to quantum chromodynamics: Light fermions in its landscape, Phys. Rev. D **109**, 086005 (2024).

[15] P. D. Mannheim, Ghost problems from Pauli–Villars to fourth-order quantum gravity and their resolution, Int. J. Mod. Phys. D **29**, 2043009 (2020).

[16] J. F. Donoghue and G. Menezes, Unitarity, stability and loops of unstable ghosts, Phys. Rev. D **100**, 105006 (2019).

[17] D. Anselmi, Fakeons, Lee-Wick models, J. High Energy Phys. 02 (2018) 141.

[18] D. Anselmi and M. Piva, A new formulation of Lee-Wick quantum field theory, J. High Energy Phys. 06 (2017) 066; D. Anselmi and M. Piva, Perturbative unitarity in Lee-Wick quantum field theory, Phys. Rev. D **96**, 045009 (2017).

[19] D. Anselmi, On the quantum field theory of the gravitational interactions, J. High Energy Phys. 06 (2017) 086.

[20] D. Anselmi, Diagrammar of physical and fake particles and spectral optical theorem, J. High Energy Phys. 11 (2021) 030.

[21] D. Anselmi, A new quantization principle from a minimally non time-ordered product, J. High Energy Phys. 12 (2022) 088.

[22] D. Anselmi, E. Bianchi, and M. Piva, Predictions of quantum gravity in inflationary cosmology: Effects of the Weyl-squared term, J. High Energy Phys. 07 (2020) 211.

[23] D. Anselmi, Dressed propagators, fakeon self-energy and peak uncertainty, J. High Energy Phys. 06 (2022) 058.

[24] D. Anselmi, Fakeons, microcausality and the classical limit of quantum gravity, Classical Quantum Gravity **36**, 065010 (2019).

[25] G. Calcagni, Classical and quantum gravity with fractional operators, Classical Quantum Gravity **38**, 165005 (2021); **38**, 169601(E) (2021).

[26] G. Calcagni and L. Rachwał, Ultraviolet-complete quantum field theories with fractional operators, J. Cosmol. Astropart. Phys. 09 (2023) 003.

[27] G. Calcagni and G. Nardelli, Representations of the fractional d'Alembertian and initial conditions in fractional dynamics, Chaos, Solitons Fractals **201**, 117401 (2025).

[28] G. Calcagni and F. Briscese, Perturbative unitarity of fractional field theories and gravity, arXiv:2603.25709.

[29] N. V. Krasnikov, Higgs boson with continuously distributed mass, Phys. Lett. B **325**, 430 (1994); N. V. Krasnikov, Unparticle as a field with continuously distributed mass, Int. J. Mod. Phys. A **22**, 5117 (2007).

[30] H. Georgi, Unparticle physics, Phys. Rev. Lett. **98**, 221601 (2007).

[31] R. E. Cutkosky, Singularities and discontinuities of Feynman amplitudes, J. Math. Phys. (N.Y.) **1**, 429 (1960); M. Veltman, Unitarity and causality in a renormalizable field theory with unstable particles, Physica **29**, 186 (1963); G. 't Hooft, Renormalization of massless Yang-Mills fields, Nucl. Phys. **B33**, 173 (1971); G. 't Hooft, Renormalizable Lagrangians for massive Yang-Mills fields, Nucl. Phys. **B35**, 167 (1971); G. 't Hooft and M. Veltman, Diagrammar, CERN report CERN-73-09; M. Veltman, *Diagrammatica. The Path to Feynman Rules* (Cambridge University Press, New York, 1994).

[32] C. G. Bollini and J. J. Giambiagi, The number of dimensions as a regularizing parameter, Nuovo Cimento Soc. Ital. Fis. **12B**, 20 (1972); C. G. Bollini and J. J. Giambiagi, Lowest order divergent graphs in ν-dimensional space, Phys. Lett. **40B**, 566 (1972); G. t Hooft and M.Veltman, Regularization and renormalization of gauge fields, Nucl. Phys. **B44**, 189 (1972); G. M. Cicuta and E. Montaldi, Analytic

renormalization via continuous space dimension, Lett. Nuovo Cimento **4**, 329 (1972).

[33] C. G. Bollini, J. J. Giambiagi, and A. Gonzáles Domínguez, Analytic regularization and the divergences of quantum field theories, Nuovo Cimento **31**, 550 (1964); E. R. Speer, On the Structure of Analytic Renormalization, J. Math. Phys. (N.Y.) **9**, 1404 (1968).

[34] G. Calcagni, Quantum scalar field theories with fractional operators, Classical Quantum Gravity **38**, 165006 (2021).

[35] C. G. Bollini and M. C. Rocca, The Wheeler propagator, Int. J. Theor. Phys. **37**, 2877 (1998); A. Plastino and M. C. Rocca, Quantum field theory, Feynman-Wheeler propagators, dimensional regularization in configuration space and convolution of Lorentz Invariant Tempered Distributions, J. Phys. Comm. **2**, 115029 (2018).

[36] D. Anselmi, The quest for purely virtual quanta: Fakeons versus Feynman-Wheeler particles, J. High Energy Phys. 03 (2020) 142.

[37] J. C. Ward, An identity in quantum electrodynamics, Phys. Rev. **78**, 182 (1950); Y. Takahashi, On the generalized Ward identity, Nuovo Cimento, **6**, 371 (1957); A. A. Slavnov, Ward identities in gauge theories, Theor. Math. Phys. **10**, 99 (1972); J. C. Taylor, Ward identities and charge renormalization of Yang-Mills field, Nucl. Phys. **B33**, 436 (1971).

[38] D. Anselmi and G. Calcagni, Classicized dynamics and initial conditions in field theories with fakeons, J. High Energy Phys. 01 (2026) 104.